Theoretical Study on Metal NMR Chemical Shifts. Electronic Mechanism of the Xe Chemical Shift

Shinji Tanaka, Manabu Sugimoto, Hajime Takashima, Masahiko Hada, and Hiroshi Nakatsuji[*,#]

Department of Synthetic Chemistry and Biological Chemistry, Faculty of Engineering, Kyoto University, Sakyo-ku, Kyoto 606-01

(Received November 21, 1995)

The ^{129}Xe chemical shifts of the complexes XeF_{2n}, $XeF_{2n-1}{}^{+}$ and XeO_nF_{6-2n} ($n = 1$—3) are studied theoretically by ab initio finite perturbation method. The first-order higher basis functions (FOBFs) are added to the standard basis set for removing the gauge-dependence. The calculated values of the Xe chemical shifts agree reasonably with the experimental values. Though the electronic configuration of Xe is the closed shell $5s^2 5p^6$, the electronic mechanism of the Xe chemical shift is shown to be the *p-mechanism*. Namely, the dominant term in the Xe chemical shift is the paramagnetic term and it is mainly governed by the Xe valence p AO contribution. Actually, as expected, the Xe chemical shifts show the U-shaped dependence on the number of the Xe valence p electrons. The diamagnetic term is small and depends linearly on the number of the ligands.

Xe is an inert atom and its electronic configuration is characterized by the closed shell configuration $4d^{10}5s^2 5p^6$, however some kinds of the Xe compounds have been found experimentally as electron-excess compounds. The data of the ^{129}Xe NMR chemical shifts have been accumulated for various Xe compounds[1] and published in review articles.[2] However, the electronic mechanism of the Xe chemical shifts is not yet clear.

In this series of studies, we have clarified the mechanisms of the NMR chemical shifts of various nuclear species.[3] They are classified into four patterns corresponding to the positions on the periodic table. The compounds of Cu, Ag, Zn, and Cd,[4,5] whose electron configurations are $d^{10}s^{1-2}p^0$ show the p-electron and d-hole mechanisms, and the compounds of Ti,[6] Nb,[7] Mn,[8] and Mo[9,10] which have open d subshells show the d-excitation mechanism. The compounds of Si, Ge,[11] Sn,[12,13] and Se[14] whose electron configurations are $s^2 p^{2-4}$ show the p-electron and p-hole mechanisms, and the compounds of Ga and In[15,16] whose electron configurations are $s^2 p^1$ show the diamagnetic mechanism. Further, the calculated chemical shifts in our previous papers agreed reasonably with the experimental values.

A problem in the calculations of the magnetic shielding constants is the gauge origin dependence and the basis set dependence. Gauge invariant atomic orbitals (GIAO)[17] and individual gauge for localized orbitals (IGLO)[18] methods are useful for avoiding this problem. As an alternative method, we have proposed the first order higher angular momentum basis function (FOBF) method, in which the FOBFs are added to the conventional gaussian basis set.[19] This method has been applied to the Se and Cd,[20] As and Sb,[21] and Ga

and In[16] compounds, and the accuracy of this method has been well examined.

In our preliminary calculations we found that the calculated Xe chemical shifts do not reproduce well the experimental values when we use only the conventional basis set. Here, we carry out the calculations of the Xe chemical shifts using larger basis sets including the FOBFs. After examining the accuracy of our calculated results, we analyze the electronic mechanism of the Xe chemical shifts. The compounds studied in this paper are XeF_{2n}, XeF_{2n-1}^{+}, and XeO_nF_{6-2n} ($n = 1, 2, 3$).

Method of Calculations

The ^{129}Xe chemical shifts are calculated by the ab initio Hartree–Fock/finite perturbation method. The details of the method were described in our previous paper.[4] For the SCF calculations, the HONDO7 program is used. The gauge origin is located at the position of the Xe nucleus.

Experimental geometries are used for the neutral molecules, XeF_{2n} ($n = 1$—3),[22] $XeOF_4$,[22] XeO_2F_2,[23] and XeO_3,[24] while the optimized geometries are used for the cationic molecules; XeF_{2n-1}^{+} ($n = 1, 2, 3$) because of the lack of the experimental geometries. For XeF^+, we use the optimized structure of the salt $XeF^+SbF_6{}^-$ instead of XeF^+ to mimic the experimental condition,[5] and the chemical shift is also calculated using the $XeF^+SbF_6{}^-$ structure. For XeF_6, we use two kinds of geometry. One is taken from a free XeF_6 molecule[22] and the other is from a part of the tetramer $(XeF_6)_4$ determined by the X-ray diffraction,[25] whose chemical shift is observed in F_5SOSF_5 at $-118\ °C$.[26] In Fig. 1, we summarize the geometries of the compounds studied in this paper.

The basis sets used in the present study are as follows. For calculating the chemical shifts, Huzinaga's basis (16s13p7d)/[7s6p2d][27] plus p,d-FOBFs (triple zeta) for the valence orbitals are used for Xe, and Pople's 6-31G[28] basis plus d-FOBFs (double zeta) are used for the atoms connected directly to Xe. Huzinaga's basis (16s13p7d)/[6s5p2d] (double zeta) plus polarization d function
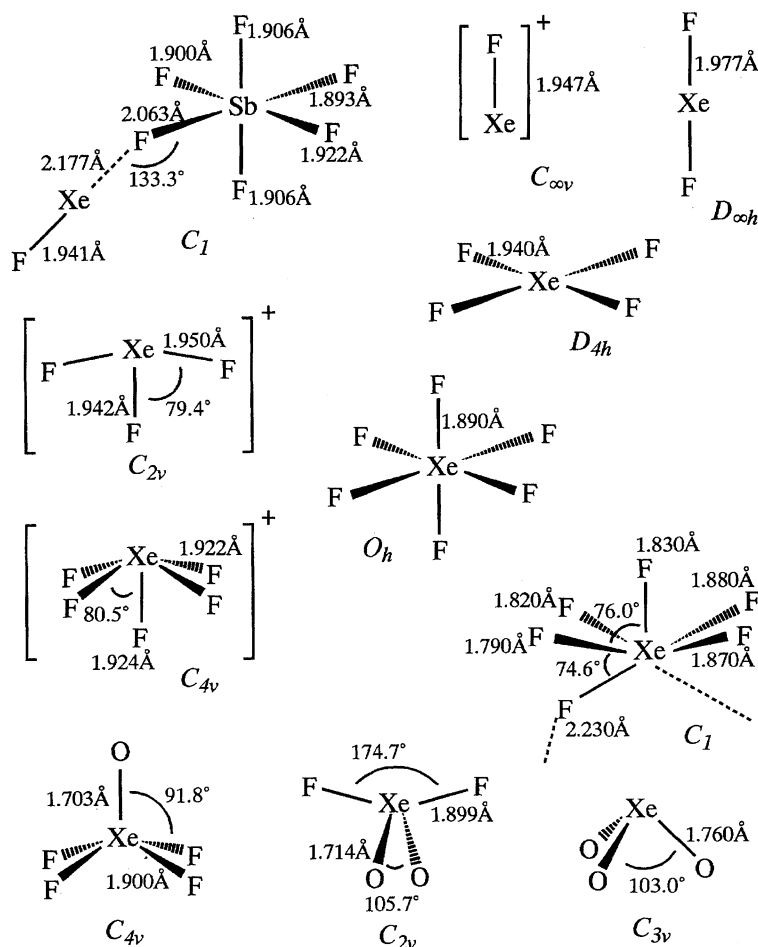
Fig. 1. The geometries of Xe compounds for calculations.

($\zeta = 0.211$)[27] are used for Sb and Pople's 6-31G[28] basis (double zeta) is used for F which is not connected directly to Xe. For optimizing geometries, we used the smaller basis set as follows. Huzinaga's basis (16s13p7d)/[6s5p3d][27] (double zeta) are used for Xe and (7s4p)/[3s2p][27] (double zeta) are used for the atoms neighboring to Xe. Only for optimizing the geometry of XeF$^+$SbF$_6^-$, Huzinaga's basis (16s13p7d)/[7s6p2d][27] (triple zeta) plus polarization d function ($\zeta = 0.297$) are used for Xe and Pople's 6-31G[28] basis (double zeta) is used for the atoms neighboring to Xe.

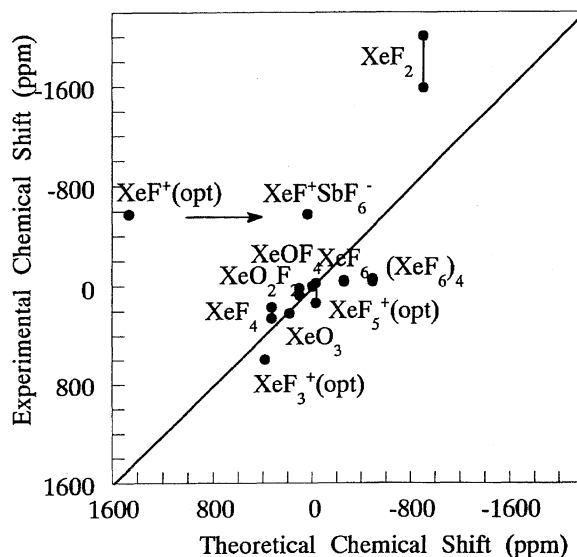The Xe chemical shift of the compound M, δ_M, is defined relative to the reference compound XeOF$_4$ as,

$$\delta_M = \sigma(\text{XeOF}_4) - \sigma(\text{M}), \qquad (1)$$

and the nuclear magnetic shielding constant σ is the sum of the diamagnetic term σ^{dia} and the paramagnetic term σ^{para} as,

$$\sigma = \sigma^{dia} + \sigma^{para}. \qquad (2)$$

In the perturbation theory, σ^{dia} and σ^{para} correspond to the first- and second-order terms, respectively.[29] It is our general result that σ^{dia} is governed by the structural factor, and σ^{para} is affected by the electronic structure of the molecule.[3]

Comparison with Experiment and Effects of the FOBF. The correlations between the calculated and experimental values of the Xe chemical shifts are shown in Fig. 2. The horizontal axis shows the calculated chemical shift and the vertical axis shows the experimental chemical shift. Therefore, the point on the 45 degree line

Fig. 2. Correlation between experimental and theoretical values of the ^{129}Xe chemical shifts of the Xe compounds.

drawn in this figure means a complete agreement between the theoretical and experimental values. In the present study, the agreement between theory and experiment is reasonably good. For XeF$^+$, the calculated chemical shift deviates largely from the observed value

when we use the optimized geometry of free XeF⁺, while the agreement is much improved when we use the geometry of the salt, XeF⁺SbF₆⁻, in the experimental condition. Experimental examinations of this findings is interesting. On the other hand, though the two geometries of XeF_6 and $(XeF_6)_4$ are different as shown in Fig. 1, the experimental chemical shifts of XeF_6 and $(XeF_6)_4$ are quite close to each other.[2] Accordingly, the calculated chemical shifts using XeF_6 and $(XeF_6)_4$ geometries are similar to each other.

Figure 3 shows the effects of the FOBFs. The chemical shifts of all the compounds move to lower field by adding the FOBFs, since the description only for σ^{para} is improved as shown below. As a result, we see a large improvement in the calculated values. For example, in XeF_3^+, the chemical shift of -657 ppm is varied to 387 ppm by adding the FOBFs, while the experimental value is 595 ppm. For XeF_2, however, the effect of the FOBF makes the deviation from the experimental value larger. We think that the difference is due to the neglect of the solvent effect.

Table 1 shows the σ^{dia} and σ^{para} terms with and without FOBFs. The σ^{dia} terms in these compounds are not much affected by the FOBFs. On the other hand, the σ^{para} terms are largely stabilized and the absolute values become larger by adding the FOBFs in all the compounds. This change of σ^{para} in the standard substance $XeOF_4$ is the smallest in all of these compounds, and therefore the chemical shifts of all the compounds move to lower field by adding the FOBFs showed in Fig. 2.

AO and MO Contributions.   The Xe nuclear magnetic shielding constants are decomposed into the core and valence contributions[3] and the result is summarized in Table 2 for all the compounds studied here. The experimental chemical shifts shown
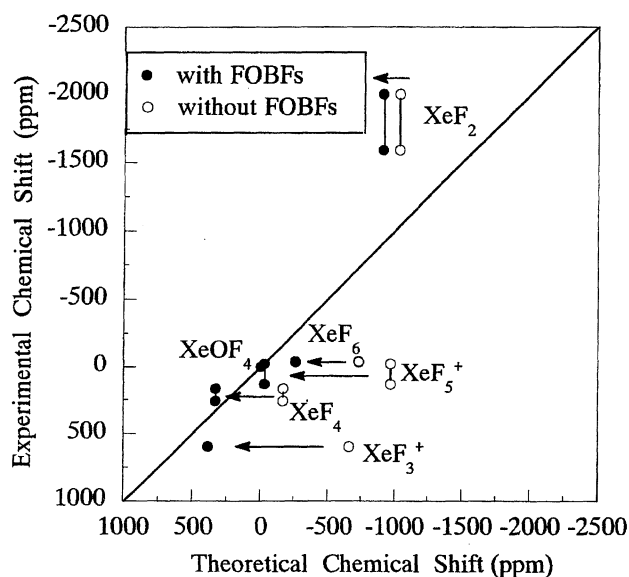

Fig. 3.   The comparison shift after adding FOBFs and before adding FOBFs.

in the last column of the table are distributed in the wide range; -2000—200 ppm. In σ^{dia}, the valence MO contribution shows the largest variation however it is within 140 ppm. On the other hand, in σ^{para}, the variation in the valence MO contribution is as large as 1200 ppm (from -3000 to -4200 ppm), while the total shifts varies in the width of 1300 ppm (from 1200 to 2500 ppm). Therefore, the

Table 1. σ^{dia}, σ^{para}, and the Chemical Shift δ of the Xe Compounds with and without the FOBFs (in ppm)

Molecule	without FOBFs				with FOBFs				
	σ^{dia}	σ^{para}	σ^{tot}	$\delta_{(XeOF_4)}$	σ^{dia}	σ^{para}	σ^{tot}	$\delta_{(XeOF_4)}$	δ_{exptl}
XeF_2	5713	-2888	2825	-1031	5710	-3216	2494	-905	$-1592/-2009$
XeF_3^{+} [a]	5750	-3300	2450	-657	5748	-4547	1201	387	595
XeF_4	5798	-3839	1959	-166	5797	-4541	1256	332	166/259
XeF_5^{+} [a]	5835	-3075	2760	-967	5834	-4220	1613	-25	$-24/132$
XeF_6 [b]	5889	-3367	2522	-729	5888	-4044	1845	-257	$-35/-45$
$XeOF_4$	5844	-4051	1793	0	5843	-4255	1588	0	0

a) Optimized geometry.   b) Monomer.

Table 2.   Diamagnetic and Paramagnetic Contributions, σ^{dia} and σ^{para}, to the Xe Nuclear Magnetic Shielding Constant σ and Their Analyses into Core and Valence MO Contributions (in ppm)

Molecule	σ^{dia}				σ^{para}				σ^{tot}		δ_{exptl}
	Core	Valence	Total	Shift	Core	Valence	Total	Shift	Total	Shift	
XeF⁺ [a]	5289	375	5663	180	-372	-5174	-5546	1291	118	1471	$-574/-911$
XeF⁺SbF₆⁻ [a]	5405	520	5925	-82	-313	-4060	-4373	118	1552	37	-574
XeF_2	5298	412	5710	133	-215	-3001	-3216	-1039	2494	-905	$-1592/-2009$
XeF_3^{+} [a]	5308	440	5748	95	-303	-4244	-4547	292	1201	387	595
XeF_4	5318	479	5797	46	-302	-4238	-4541	286	1256	332	166/259
XeF_5^{+} [a]	5327	506	5834	9	-282	-3939	-4220	-35	1613	-25	$-24/132$
XeF_6 [b]	5338	550	5888	-45	-272	-3772	-4044	-211	1845	-257	$-35/-45$
XeF_6 [c]	5338	550	5888	-45	-254	-3554	-3808	-447	2080	-492	$-39/-61$
$XeOF_4$	5329	514	5843	0	-283	-3972	-4255	0	1588	0	0
XeO_2F_2	5320	478	5798	45	-287	-4028	-4315	60	1483	105	17/171
XeO_3	5311	440	5750	93	-290	-4060	-4349	94	1401	187	217

a) Optimized geometry.   b) The geometry is taken from a monomer of XeF_6.   c) The geometry is taken from a tetramer of XeF_6.

Xe chemical shifts are determined by the variation in the valence MO contribution to σ^{para}.

Table 3 shows the diamagnetic and paramagnetic contributions partitioned into the contributions of the s, p, and d orbitals of Xe and the ligands. The largest variation due to the substitution of the ligand is found on the Xe p AO contribution of σ^{para}, whose range is about 1200 ppm. Though the second largest variation is seen for the Xe d AO contribution to σ^{para}, the width 450 ppm is smaller than that of the p AO, 1200 ppm. The ligand contributions themselves are small. As shown in Table 2, we already know that the valence electron contribution is dominant. Therefore, from Tables 2 and 3 we conclude that the Xe valence p AO contribution to σ^{para} is the dominant origin of the Xe chemical shifts. We note that the s AO contribution in σ^{para} vanishes identically, since the s AO does not have an angular momentum.

In conclusion, the dominant mechanism of the Xe chemical shift is the *p-mechanism* in σ^{para}. In the following sections, we analyze the mechanism of the Xe chemical shifts in more detail.

Detailed Analysis

A. Diamagnetic Contribution. For the metal chemical shifts studied so far, the diamagnetic contribution has been found to be relatively unimportant, except for an interesting case of the Ga and In chemical shifts for which the diamagnetic term is dominant. When the ligand halogen becomes heavy as Br and I, the spin-orbit (SO) effects becomes very important as well.[16] As shown in Table 2, the diamagnetic contribution is small in the present case and does not affect the total values. However, the diamagnetic terms have a clear relationship with the number of ligands.[4] Figure 4 shows this relationship. We see a beautiful linear relationship between the diamagnetic term and the number of the ligands. This origin is shown as follows.

The diamagnetic term is determined only by the structural factor. Flygare and Goodisman[30] have reported that the diamagnetic term of the nucleus M is approximately expressed as

$$\sigma^{\text{dia}} = \sigma^{\text{dia}}(\text{free atom M}) + \frac{e^2}{3mc^2}\sum_\alpha \frac{Z_\alpha}{r_\alpha} \qquad (3)$$

Fig. 4.   Correlation between the number of F and O atoms and diamagnetic terms.

where σ^{dia} (free atom M) is the diamagnetic shielding constant of the free atom M, α runs over all nuclei except for M, Z_α is the atomic number of the nuclei α, and r_α is the distance between M and α. If the distance r_α is a constant over a class of the compounds, σ^{dia} should be proportional to the number of the ligands shown in Fig. 4. Previously,[4] we have presented a simpler expression like the Pascal-rule,

$$\sigma^{\text{dia}} = \sigma^{\text{dia}}(\text{Xe}) + \sum_L n_L \sigma^{\text{dia}}(\text{L}) \qquad (4)$$

Though this formula was derived from the analysis of the calculated result, it can also be derived from Eq. 3 by assuming that r_α is constant for each ligand. In Eq. 4, $\sigma^{\text{dia}}(\text{Xe})$ is the sum of the Xe AO contributions, $\sigma^{\text{dia}}(\text{L})$ the ligand contribu-

Table 3.   Diamagnetic and Paramagnetic Contributions, σ^{dia} and σ^{para}, to the Xe Nuclear Magnetic Shielding Constant σ Analysed into the s,p,d AO Contributions and the Ligand Contributions (in ppm)

Molecule	$\sigma^{\text{dia}}(\text{Xe})$				$\sigma^{\text{dia}}(\text{L})$	$\sigma^{\text{para}}(\text{Xe})^{a)}$			$\sigma^{\text{para}}(\text{L})$	σ^{tot}
	s	p	d	tot	tot	p	d	tot	tot	
XeF+ b)	2572	2012	1034	5618	46	−5530	15	−5514	−31	118
XeF+SbF6− b)	2572	2011	1035	5618	307	−4196	−76	−4272	−89	1552
XeF2	2572	2011	1035	5618	92	−2986	−159	−3145	−70	2494
XeF3+ b)	2572	2002	1035	5610	137	−4208	−237	−4446	−100	1200
XeF4	2574	1998	1037	5609	187	−4020	−375	−4396	−143	1256
XeF5+ b)	2572	1992	1037	5600	233	−3544	−505	−4049	−170	1613
XeF6 c)	2578	1984	1037	5598	290	−3299	−520	−3819	−224	1845
XeF6 d)	2573	1987	1037	5597	291	−3055	−531	−3586	−222	2080
XeOF4	2573	1990	1037	5600	242	−3570	−503	−4074	−180	1588
XeO2F2	2571	1994	1037	5602	196	−3722	−454	−4176	−140	1483
XeO3	2570	1999	1037	5606	144	−3837	−416	−4253	−96	1401

a) The Xe s AO contribution is identically zero because the s AO does not have an angular momentum.   b) Optimized geometry.   c) The geometry is taken from a monomer of XeF6.   d) The geometry is taken from a tetramer of XeF6.
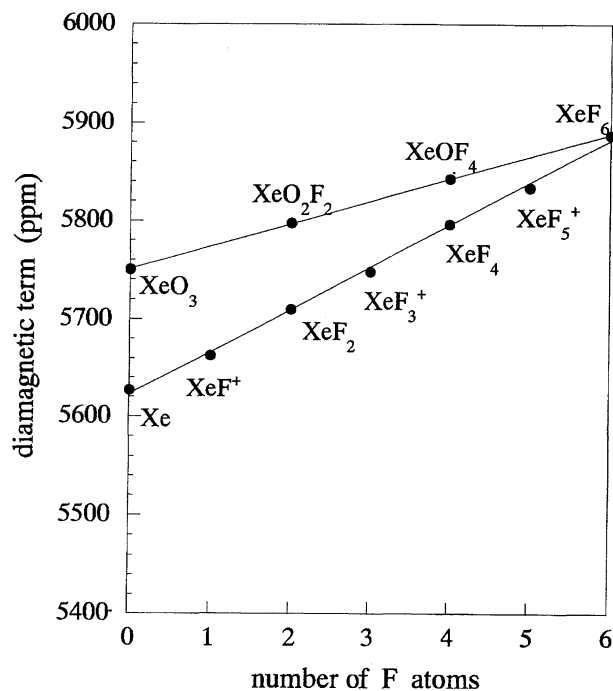
tion, and n_L the number of ligands L. From the values shown in Table 3, $\sigma^{\text{dia}}(\text{Xe})$ and $\sigma^{\text{dia}}(\text{F})$ in Eq. 4 are calculated to be 5627 ppm and 42 ppm, respectively. Equation 4 holds to a good approximation for the diamagnetic term in the present case.

B. Electronic Structure.   Before analyzing the paramagnetic term, we should describe briefly about the electronic structure of the Xe compound.

The Xe–F bond in XeF^+ is formed from the vacant $2p_\sigma$ orbital of F^+ and the doubly occupied 5p orbital of Xe. On the other hand, the F–Xe–F bond in XeF_2 is the well-known 3-center-4-electron bond. In other compounds, XeF_{2n} and $\text{XeF}_{2n-1}{}^+$, the Xe–F and F–Xe–F bonds have similar natures as those in XeF^+ and XeF_2, respectively. Thus, all bondings in these compounds consist of the 5p orbital of Xe and the 2p orbital of F. The Xe–O bond may be analogous to that of XeF^+ since O and F^+ are isoelectronic and from the bonding nature it is polarized as Xe^+–O^-.

The geometries of these compounds shown in Fig. 1 are understood from these bonding nature. In XeF_2, XeF_4, and XeF_6, there are one, two, and three F–Xe–F bonds, respectively, and their geometries are $D_{\infty h}$, D_{4h}, and O_h, respectively. In $\text{XeF}_3{}^+$, there are one F–Xe–F bond and one XeF^+ bond. The angle between these bonds are less than 90°, because the lone pair existing in the backwards of the XeF^+ bond exerts the atomic dipole (AD)[31] force on Xe which is larger than the exchange (EC)[31] force due to the Xe–F bond. The geometry of $\text{XeF}_5{}^+$ is understood similarly to $\text{XeF}_3{}^+$. On the other hand, the angle of O–Xe–F in XeOF_4 is larger than 90°. These geometries are due to the charge polarization along the Xe–F and Xe–O bond. In XeOF_4, the axial O atom has the charge as large as -0.99, and the F atom -0.61 (see Table 4).

C. Paramagnetic Contribution.   As shown in Tables 2 and 3, the valence p AO contribution to σ^{para} is dominant in the ^{129}Xe chemical shifts. In order to analyze this term more clearly we use the expression of σ^{para} in the perturbation theory.

$$(\sigma^{\text{para}})_{xy} = -\frac{m_o e^2}{8\pi m^2} \sum_n \frac{1}{E_n - E_0}$$

$$\left[\left\langle 0 \left| \sum_v l_{xv} \right| n \right\rangle \left\langle n \left| \sum_v \frac{l_{yv}}{r_v{}^3} \right| 0 \right\rangle + c.c \right] \quad (5)$$

where l_{xv} is an angular momentum operator around the x axis, and $|o>$ and $|n>$ the wave functions for the ground and excited states, respectively. $c.c$ denotes complex conjugate. Since Eq. 5 includes angular momentum operators, the p and d atomic orbitals of Xe mainly contribute to σ^{para}. Table 4 shows the Malliken population analysis. Since we already know that the Xe valence p orbital is important for the chemical shifts, we analyze the p AO population. The population of the 5p orbitals varies in the range of 1.7—4.5. From XeF^+ to XeF_6, by increasing the number of ligand F, the electron population of $\text{Xe}(5p)$ decreases, since F is more electronegative than Xe. On the other hand, from XeF_6 to XeO_3, by replacing fluorine with oxygen, the electron population of $\text{Xe}(5p)$ increases, due to the electronegativity difference between O and F.

In Fig. 5, the paramagnetic values are plotted against the Xe 5p orbital population. We see a U-shaped relationship between these quantities and the bottom exists around $x=3$. This is a general tendency when the chemical shifts depend on the number of the p electrons. The angular momentum of the p orbital is maximum when the occupancy is just half, and the empty and fully occupied p orbitals give no angular momentum at all. We call this mechanism 'p-mechanism'.[3] The details have been discussed in a previous paper.[13] The results of the neutral and cationic species seem to be on different curves.

We have previously shown that after some approximations,[32] we can express the paramagnetic terms as

$$\sigma^{\text{para}} = -\text{const.} \frac{1}{\Delta E} \left\langle \frac{1}{r^3} \right\rangle P \left\{ \frac{3}{2} - \frac{1}{6}(I-3)^2 + \frac{1}{6}A^2 \right\} \quad (6)$$

where

$$I = D_{xx} + D_{yy} + D_{zz}, \quad (7)$$

$$A = D_{zz} - \frac{1}{2}(D_{xx} + D_{yy}), \quad (8)$$

Table 4.   Valence AO Populations and the Charges of Xe and Ligand Atoms

Molecule	Xe				F				O				$\sigma^{\text{para g)}}$
	s(5s)	p(5p)	$d^{\text{a)}}$	Charge[c]	s(2s)	p(2p)	$d^{\text{a)}}$	Charge[e]	s(2s)	p(2p)	$d^{\text{a)}}$	Charge[e]	
XeF^+ [b]	1.163	4.618	0.764	+1.347	1.948	5.297	0.109	−0.347	—	—	—	—	−5546
$\text{XeF}^+\text{SbF}_6{}^-$ [b]	1.341	4.503	0.610	+1.287	1.928	5.482	0.117	−0.519	—	—	—	—	−4373
XeF_2	1.342	4.506	0.699	+1.192	1.911	5.574	0.119	−0.596	—	—	—	—	−3216
$\text{XeF}_3{}^+$ [b]	1.289	3.514	0.633	+2.297[f]	1.943	5.376	0.100	−0.432[f]	—	—	—	—	−4547
XeF_4	1.388	3.122	0.837	+2.371	1.921	5.556	0.123	−0.593	—	—	—	—	−4541
$\text{XeF}_5{}^+$ [b]	1.227	2.442	0.741	+3.321[f]	1.955	5.384	0.127	−0.464[f]	—	—	—	—	−4220
XeF_6 [c]	1.479	1.747	0.721	+3.736	1.934	5.564	0.133	−0.623	—	—	—	—	−4044
XeF_6 [d]	1.250	1.994	0.774	+3.772[f]	1.942	5.554	0.132	−0.247[f]	—	—	—	—	−3808
XeOF_4	1.239	2.303	0.762	+3.436	1.932	5.556	0.130	−0.609	2.071	4.836	0.094	−0.999	−4255
XeO_2F_2	1.173	2.650	0.752	+3.182	1.926	5.564	0.123	−0.605	2.051	4.849	0.089	−0.986	−4315
XeO_3	1.150	3.079	0.778	+2.757	—	—	—	—	2.032	4.816	0.078	−0.919	−4349

a) Polarization d orbital.   b) Optimized geometry.   c) The geometry is taken from a monomer of XeF_6.   d) The geometry is taken from a tetramter of XeF_6.   e) The net charge of this atom.   f) This charge is the average of the charge of corresponding ligands.   g) in ppm.
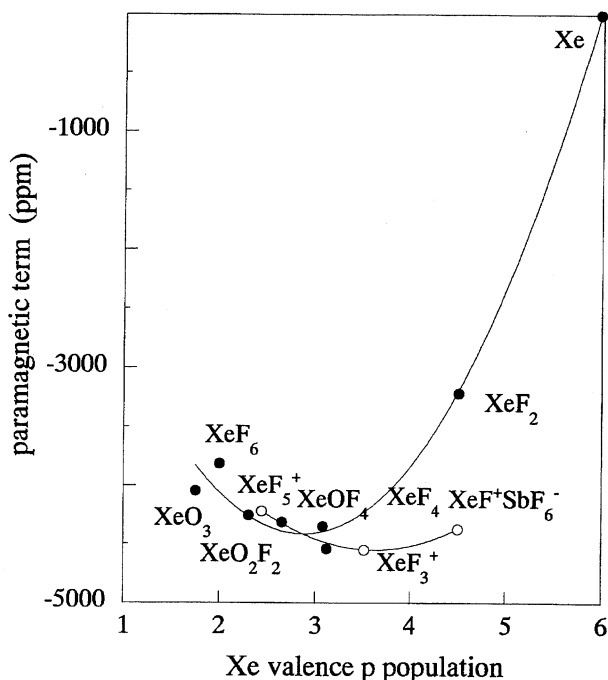
Fig. 5.   Correlation between the valence p population of Xe
atom and paramagnetic term.

and ΔE is the average excitation energy, $\langle 1/r^3 \rangle p$ is the average value of r^{-3} over the p_x, p_y, and p_z orbitals of Xe, D_{xx} denotes the density matrix of p_x orbital, I is the isotropic density and A is the anisotropic one. This equation shows that σ^{para} depends on the density I in a U-shape and the bottom is located at $I=3$ assuming that the change in A is small. Our calculated results support the above formula.

Conclusion

The ^{129}Xe chemical shifts of the Xe compounds XeF_{2n}, XeF_{2n-1}^+, and XeO_nF_{6-2n} ($n=1$—3) are calculated by ab initio molecular orbital method for clarifying the electronic mechanism. The FOBFs are added to the valence part of the basis set. The results of the present study are as follows.

(1) The calculated values of the chemical shifts agree with the experimental ones when we add the FOBFs to the standard basis set. Only when we use the geometry of the salt $XeF^+SbF_6^-$, we can reproduce the experimental Xe chemical shift of XeF^+.

(2) The paramagnetic term is dominant in the Xe chemical shifts and arises from the valence p AO contribution. Thus, the Xe chemical shift is due to the *p-mechanism* within our four patterns.

(3) The change in the diamagnetic term is small. It depends linearly on the number of ligands.

(4) The paramagnetic term and the Xe 5p population show a *U-shape* relationship, which can be derived when the mechanism of the chemical shift is *p-mechanism*.

References

1)   J. Schrobilgen, H. Holloway, P. Granger, and C. Brevard, *Inorg. Chem.*, **17**, 980 (1978).

2)   R. K. Harris, J. D. Kennedy, and W. McFarlane, in "NMR and the Periodic Table," ed by R. K. Harris and B. E. Mann, Academic Press, New York (1978), p. 439; J. D. Kennedy and W. McFarlane, in "Multinuclear NMR," ed by J. Mason, Plenum, New York (1987), p. 463.

3)   H. Nakatsuji, in "Nuclear Magnetic Shieldings and Molecular Structure," ed by J. A. Tossell, Kluwer, Dortrecht (1993), p. 263.

4)   H. Nakatsuji, K. Kanda, K. Endo, and T. Yonezawa, *J. Am. Chem. Soc.*, **106**, 4653 (1984).

5)   H. Nakatsuji, T. Nakao, and K. Kanda, *Chem. Phys.*, **115**, 25 (1987).

6)   H. Nakatsuji and T. Nakao, *Chem. Phys. Lett.*, **167**, 571 (1990).

7)   M. Sugimoto, M. Kanayama, and H. Nakatsuji, *J. Phys. Chem.*, **96**, 4375 (1992).

8)   K. Kanda, H. Nakatsuji, and T. Yonezawa, *J. Am. Chem. Soc.*, **106**, 5888 (1984).

9)   H. Nakatsuji and M. Sugimoto, *Inorg. Chem.*, **29**, 1221 (1990).

10)   H. Nakatsuji, M. Sugimoto, and S. Saito, *Inorg. Chem.*, **29**, 3095 (1990).

11)   H. Nakatsuji and T. Nakao, *Int. J. Quantum Chem.*, **49**, 279 (1994).

12)   H. Nakatsuji, T. Nakao, and T. Inoue, *Chem. Phys. Lett.*, **167**, 111 (1990).

13)   H. Nakatsuji, T. Inoue, and T. Nakao, *J. Phys. Chem.*, **96**, 7953 (1992).

14)   H. Nakatsuji, T. Higashioji, and M. Sugimoto, *Bull. Chem. Soc. Jpn.*, **66**, 3235 (1993).

15)   M. Sugimoto, M. Kanayama, and H. Nakatsuji, *J. Phys. Chem.*, **97**, 5868 (1993).

16)   H. Takashima, M. Hada, and H. Nakatsuji, *Chem. Phys. Lett.*, **235**, 13 (1995).

17)   R. Ditchfield, *Mol. Phys.*, **27**, 789 (1974).

18)   W. Kutzelnigg, *Isr. J. Chem.*, **19**, 193 (1980); M. Schindler and W. Kutzelnigg, *J. Chem. Phys.*, **76**, 1919 (1982); M. Schindler and W. Kutzelnigg, *J. Am. Chem. Soc.*, **105**, 1360 (1983); M. Schindler and W. Kutzelnigg, *Mol. Phys.*, **48**, 781 (1983).

19)   M. Sugimoto and H. Nakatsuji, *J. Chem. Phys.*, **102**, 285 (1995).

20)   T. Higashioji, M. Hada, M. Sugimoto, and H. Nakatsuji, *Chem. Phys.*, in press.

21)   H. Takashima, M. Hada, and H. Nakatsuji, *J. Phys. Chem.*, **99**, 13 (1995).

22)   J. H. Callomon, E. Hirota, K. Kuchitsu, W. J. Lafferty, A. Maki, and C. S. Pote, "Landort–Börnstein New Series Supplement II/7," ed by K. -H. Hellwege and A. M. Hellwege, Springer, Berlin (1987).

23)   S. W. Peterson, R. D. Willett, and J. L. Huston, *J. Chem. Phys.*, **59**, 453 (1973).

24)   D. H. Templeton, A. Zalkin, J. D. Forrester, and S. M. Williamson, *J. Am. Chem. Soc.*, **85**, 817 (1963).

25)   R. D. Burbank and G. R Jones, *J. Am. Chem. Soc.*, **96**, 43 (1974).

26)   K. Seppelt and H. H. Rupp, *Z. Anorg. Allg. Chem.*, **409**, 331 (1974).

27)   S. Huzinaga, J. Andzelm, M. Klobukowski, E. RadzioAndzelm, Y. Sakai, and H. Tatewaki, "Gaussian Basis-Sets for Molecular Calculations," Elsevier, Amsterdam (1984).

28)   W. J. Hehre, R. Ditchfield, and J. A. Pople, *J. Chem. Phys.*, **56**, 2257 (1972).

29)   N. F. Ramsey, *Phys. Rev.*, **77**, 567 (1950); **78**, 699 (1950).
30)   W. H. Flygare and J. Goodisman, *J. Chem. Phys.*, **49**, 3122 (1968).

31)   H. Nakatsuji, *J. Am. Chem. Soc.*, **95**, 345 (1973).
32)   M. Karplus and T. P. Das, *J. Chem. Phys.*, **34**, 1683 (1961).